Voltage-Behind-Reactance Model of Six-Phase Synchronous Machine Considering Stator Mutual Leakage Inductance

Navid Amiri, Seyyedmilad Ebrahimi, Juri Jatskevich and Hermann W. Dommel

***Abstract*—Six-phase machines and the challenge of interfacing them with power electronics devices and inductive networks have always been an interesting topic of research. Coupled Circuit Phase Domain (CCPD) model of the machine has been an alternative to the conventional *qd0* equivalent circuit to address the machine interfacing issue. This paper presents another suitable alternative in the form of a Voltage-Behind-Reactance (VBR) model of the machine. Similar to the CCPD model, the VBR model can also be interfaced with any kind of network without using any snubber circuits. At the same time The VBR model achieves better numerical efficiency compared with the CCPD model due to reduced size of the system matrices. The machine model is simulated in a single-phase to ground fault scenario while being connected to a 6 phase grid. The presented model also considers machine mutual leakage inductances which are shown to have considerable effects on the simulation results.**

***Keywords*: Multi phase machines, voltage behind reactance, machine modeling, simulation.**

I. INTRODUCTION

MODELING of rotating electrical machines for studying the system transients has been an active research area for many decades [1], wherein many models have been proposed for the electromagnetic transient programs (EMTP) [2] and the state-variable (SV) -based programs [3], [4]. Electrical machines with high number of phases (more than three) on the stator in addition to having reduced power per phase also open the possibility for fault tolerant operation [5]. Six phase synchronous machines were introduced to overcome the issue of high stator current in high power generators. This makes the six-phase synchronous machine a suitable choice for ships, aircraft, and vehicles where high reliability is of critical importance [6]-[7]. With the modern variable speed high power drives, multi-phase machines are also playing an increasing role in overcoming the current limitation issues of semiconductor devices used in power electronic converters [8] [9].

The coupled circuit phase domain (CCPD) [10] and conventional *qd* [11], [12] models have been used for steady state and transient analysis of multi-phase machines. In six-phase machines, the stator is typically formed as two sets of three phase windings. The CCPD model is established based on the magnetically-coupled circuits of the stator and rotor windings [13]. The advantage of such representation is that the stator and rotor circuits can be directly interfaced with any external network, provided that the simulation program where the model is developed allows the user to implement variable inductances. In addition to the stator, the rotor will typically have several equivalent damper windings and a field winding, all of which results in increasing the size of the machine's inductance matrix. Moreover, since this model will have (variable) rotor-position-dependent self and mutual inductances, the entire machine's inductance matrix will also be variable. The changing inductances result in a model that is computationally very expensive for either EMTP or SV transient simulation programs, as the model parameters have to be recalculation at each time step.

The synchronous machine *qd* models are typically expressed in the rotating rotor reference frame [14], [15], where the equivalent circuit is derived in two *qd* planes both rotating with the same rotor speed. Moreover, the dual *qd* plane circuits have cross-coupling between each of the four axes due to the angle shift between the two three-phase sets. As expected, this formulation achieves a constant parameter model in transformed *qd* variables and a corresponding numerically efficient implementation of the model. However, similar to the conventional three-phase *qd* models [16], the six-phase *qd* model is difficult to interface with the external inductive power networks which are typically represented in physical variables and coordinates.

This paper extends the voltage behind reactance (VBR) formulation that has been proposed for the three-phase machines for both EMTP and SV transient simulation [17], [18] programs to the six-phase synchronous machine. The machine's equations in dual *qd* plane are re-arranged to provide a standard state-space model with the rotor flux linkages as the state variables, stator currents as inputs and sub-transient stator voltages as outputs. The equivalent sub-transient back emfs are first expressed in dual *qd* plane and then transformed into the six-phase *abc1abc2* coordinates. Moreover, the model takes into account the mutual leakage inductances between the two three-phase stator winding sets [14] which are shown to have a significant effect on the machine transients. The model achieves a direct and convenient interface of the stator equivalent circuit with arbitrary external networks, which is particularly useful for investigating the machine-converter transients. The new

This work was supported by the Natural Science and Engineering Research Council (NSERC) of Canada under the Discovery Grant

Paper submitted to the International Conference on Power Systems Transients (IPST2015) in Cavtat, Croatia June 15-18, 2015

model is demonstrated on an example six-phase synchronous generator system that feeds a six phase grid through an inductive line. The proposed six-phase VBR model is shown to produce very accurate simulation results and outperform the conventional *qd* and CCPD models in terms of simulation speed.

II. VBR Formulation And Equivalent Circuit

This paper models a six phase synchronous machine with two sets of symmetric three phase windings on the stator. The stator windings are arranged with a 30 degree displacement between the three phase sets. The rotor is salient and has two damper windings along the rotor *qd* axes and a field winding along d axis [14].

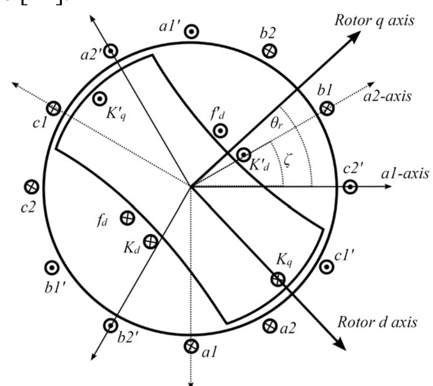

Fig. 1. Two pole salient rotor six-phase synchronous machine with 30 degree phase shift between the two three-phase set.

Having two sets of three phase windings on the stator, two separate transformations to the rotor frame are required for each three phase winding. This will create a dual plane structure, each representing one three phase set and both rotating with the same speed as the rotor. Due to the angle shift between the three phase windings, the parameters on each axis in one plane have magnetic coupling with both axes of the other plane. This coupling is represented by mutual leakage inductances in the machine's equivalent circuit. Similar to a conventional three phase synchronous machine, the six phase machine model is based on the equivalent circuit in the rotor reference frame using the following transformation.

$$\mathbf{f}_{dq012} = \overline{\mathbf{K}}(\theta_r)\mathbf{f}_{abc1abc2} \tag{1}$$

where

$$\mathbf{f}_{abc1abc2} = [f_{a1}, f_{b1}, f_{c1}, f_{a2}, f_{b2}, f_{c2}, f_{kd}, f_{kq}, f_{fd}]^T \tag{2}$$

$$\mathbf{f}_{dq012} = [f_{d1}, f_{q1}, f_{01}, f_{d2}, f_{q2}, f_{02}, f_{kd}, f_{kq}, f_{fd}]^T \tag{3}$$

$$\overline{\mathbf{K}}(\theta_r) = \text{diag}\,[\mathbf{K}(\theta_r), \mathbf{K}(\theta_r - \zeta), \mathbf{I}_{3\times 3}] \tag{4}$$

where **K** is the Clark's transformation matrix.

In Fig. 2. L_{lm} and L_{ldq} are the mutual leakage inductances between the conductors of each three phase set [14]. These mutual inductance is the result of the magnetic flux that does not cross the air gap and couples the conductors of each three phase sets in the same stator slot. The mutual leakage inductances for two three-phase sets with ζ degree shift are defined as:

$$L_{lm} = L_{la1a2}\cos\zeta + L_{la1b2}\cos(\zeta + \frac{2\pi}{3}) + L_{la1c2}\cos(\zeta - \frac{2\pi}{3}), \tag{5}$$

$$L_{ldq} = L_{la1a2}\sin\zeta + L_{la1b2}\sin(\zeta + \frac{2\pi}{3}) + L_{la1c2}\sin(\zeta - \frac{2\pi}{3}). \tag{6}$$

where L_{la1a2}, L_{la1b2} and L_{la1c2} are the actual leakage inductances which are present mostly in the stator slots between the conductors of one three-phase set and each of the conductors on the other three phase set. In a symmetric winding configuration the following relation can be considered:

$$L_{a1a2} = L_{b1b2} = L_{c1c2}\,, L_{a1b2} = L_{b1c2} = L_{c1a2}\,,$$
$$L_{a1c2} = L_{b1a2} = L_{c1b2}\,. \tag{7}$$

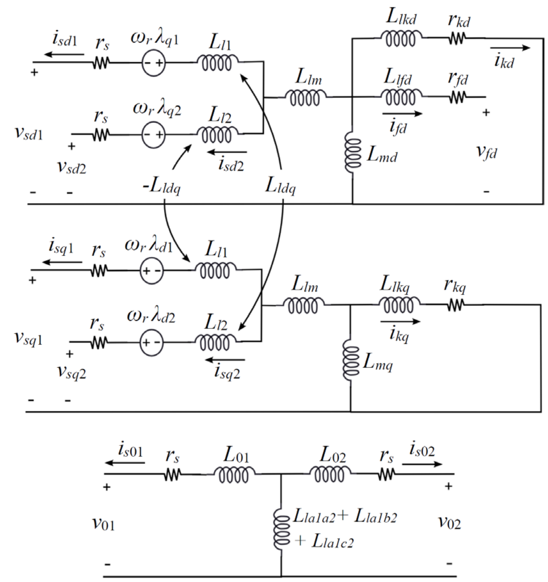

Fig. 2. Dual plane *qd0* equivalent circuit of a six-phase machine in rotor reference frame.

It should be noted that the zero sequence circuit is not considered in the VBR formulation due to the fact that the VBR model is implemented in a six-phase phase domain system with no ground connection. Based on the equivalent circuit in Fig.1. the following stator voltage equation can be defined:

$$v_{sd1} = -r_s i_{sd1} - \omega_r \lambda_{sq1} + p\lambda_{sd1}\,, \tag{8}$$

$$v_{sq1} = -r_s i_{sq1} + \omega_r \lambda_{sd1} + p\lambda_{sq1}\,, \tag{9}$$

$$v_{sd2} = -r_s i_{sd2} - \omega_r \lambda_{sq2} + p\lambda_{sd2}\,, \tag{10}$$

$$v_{sq2} = -r_s i_{sq2} + \omega_r \lambda_{sd2} + p\lambda_{sq2}\,. \tag{11}$$

In (8)-(11) the stator flux vector on both qd planes can be defined as following:

$$\lambda_{sd1} = \lambda_{md} - L_{lm}(i_{sd1} + i_{sd2}) - L_l i_{sd1} - L_{ldq} i_{sq2}\,, \tag{12}$$

$$\lambda_{sq1} = \lambda_{mq} - L_{lm}(i_{sq1} + i_{sq2}) - L_l i_{sq1} + L_{ldq} i_{sd2}\,, \tag{13}$$

$$\lambda_{sd2} = \lambda_{md} - L_{lm}(i_{sd1} + i_{sd2}) - L_l i_{sd2} + L_{ldq} i_{sq1}\,, \tag{14}$$

$$\lambda_{sq2} = \lambda_{mq} - L_{lm}(i_{sq1} + i_{sq2}) - L_l i_{sq2} - L_{ldq} i_{sd1}\,, \tag{15}$$

where the magnetizing flux is defined as:

$$\lambda_{md} = L''_{md}\left(\frac{\lambda_{kd}}{L_{lkd}} + \frac{\lambda_{fd}}{L_{lfd}} - (i_{sd1} + i_{sd2})\right), \tag{16}$$

$$\lambda_{mq} = L''_{mq}\left(\frac{\lambda_{kq}}{L_{lkq}} - (i_{sq1} + i_{sq2})\right). \tag{17}$$

In (16)-(17) the sub-transient inductances are defined as:

$$L''_{md} = \left(\frac{1}{L_{md}} + \frac{1}{L_{lkd}} + \frac{1}{L_{lfd}}\right)^{-1}, \quad L''_{mq} = \left(\frac{1}{L_{mq}} + \frac{1}{L_{lkq}}\right)^{-1}. \tag{18}$$

According to the machine equivalent circuit and by using (16)-(17), the state space equations can be expressed as the rotor flux vector.

$$p\lambda_{kd} = \frac{r_{kd}}{L_{lkd}}\left(\left(\frac{L''_{md}}{L_{lkd}} - 1\right)\lambda_{kd} + L''_{md}\frac{\lambda_{fd}}{L_{lfd}} - L''_{md}(i_{sd1} + i_{sd2})\right), \tag{19}$$

$$\begin{aligned} p\lambda_{fd} = {} & \frac{r_{fd}}{L_{lfd}}\left(\left(\frac{L''_{md}}{L_{lfd}} - 1\right)\lambda_{fd} + L''_{md}\frac{\lambda_{kd}}{L_{lkd}} - L''_{md}(i_{sd1} + i_{sd2})\right) \\ & + v_{fd} \end{aligned}, \tag{20}$$

$$p\lambda_{kq} = \frac{r_{kq}}{L_{lkq}}\left(\left(\frac{L''_{mq}}{L_{lkq}} - 1\right)\lambda_{kq} + L''_{mq}(i_{sq1} + i_{sq2})\right). \tag{21}$$

By substituting the stator flux in (8)-(11) with the ones from (12)-(15) and (16)-(17), the stator voltage equations can be re-written in the following form:

$$\begin{bmatrix} v_{sd1} \\ v_{sq1} \\ v_{sd2} \\ v_{sq2} \end{bmatrix} = -r_s \begin{bmatrix} i_{sd1} \\ i_{sq1} \\ i_{sd2} \\ i_{sq2} \end{bmatrix} - \mathbf{L}'' \begin{bmatrix} i_{sd1} \\ i_{sq1} \\ i_{sd2} \\ i_{sq2} \end{bmatrix} + \begin{bmatrix} e''_{sd1} \\ e''_{sq1} \\ e''_{sd2} \\ e''_{sq2} \end{bmatrix} \tag{22}$$

where the sub-transient inductance matrix is defined as:

$$\mathbf{L}'' = \begin{bmatrix} L_l + L''_{md} + L_{lm} & 0 & L''_{md} + L_{lm} & L_{ldq} \\ 0 & L_l + L''_{mq} + L_{lm} & -L_{ldq} & L''_{mq} + L_{lm} \\ L''_{md} + L_{lm} & -L_{ldq} & L_l + L''_{md} + L_{lm} & 0 \\ L_{ldq} & L''_{mq} + L_{lm} & 0 & L_l + L''_{mq} + L_{lm} \end{bmatrix} \tag{23}$$

and the sub-transient back-emf voltages as:

$$\begin{aligned} e''_{d1} = {} & -\omega_r \lambda''_{q1} + \left(\frac{r_{kd}L''^2_{md}}{L^3_{lkd}} - \frac{r_{kd}L''_{md}}{L^2_{lkd}} + \frac{r_{fd}L''^2_{md}}{L_{lkd}L^2_{lfd}}\right)\lambda_{kd} \\ & + \left(\frac{r_{fd}L''^2_{md}}{L^3_{lfd}} - \frac{r_{fd}L''_{md}}{L^2_{lfd}} + \frac{r_{kd}L''^2_{md}}{L_{lfd}L^2_{lkd}}\right)\lambda_{fd} \\ & - \left(\frac{r_{kd}L''^2_{md}}{L^2_{lkd}} + \frac{r_{fd}L''^2_{md}}{L^2_{lfd}}\right)(i_{sd1} + i_{sd2}) + v_{fd} \end{aligned}, \tag{24}$$

$$\begin{aligned} e''_{q1} = {} & \omega_r \lambda''_{d1} + \frac{r_{kq}L''_{mq}}{L^2_{lkq}}\left(\frac{L''_{mq}}{L_{lkq}} - 1\right)\lambda_{kq} \\ & - \frac{r_{kq}L''^2_{mq}}{L^2_{lkq}}(i_{sq1} + i_{sq2}) \end{aligned}, \tag{25}$$

$$\begin{aligned} e''_{d2} = {} & -\omega_r \lambda''_{q2} + \left(\frac{r_{kd}L''^2_{md}}{L^3_{lkd}} - \frac{r_{kd}L''_{md}}{L^2_{lkd}} + \frac{r_{fd}L''^2_{md}}{L_{lkd}L^2_{lfd}}\right)\lambda_{kd} \\ & + \left(\frac{r_{fd}L''^2_{md}}{L^3_{lfd}} - \frac{r_{fd}L''_{md}}{L^2_{lfd}} + \frac{r_{kd}L''^2_{md}}{L_{lfd}L^2_{lkd}}\right)\lambda_{fd} \\ & - \left(\frac{r_{kd}L''^2_{md}}{L^2_{lkd}} + \frac{r_{fd}L''^2_{md}}{L^2_{lfd}}\right)(i_{sd1} + i_{sd2}) + \frac{L''_{md}}{L_{lfd}}v_{fd} \end{aligned}, \tag{26}$$

$$\begin{aligned} e''_{q2} = {} & \omega_r \lambda''_{d2} + \frac{r_{kq}L''_{mq}}{L^2_{lkq}}\left(\frac{L''_{mq}}{L_{lkq}} - 1\right)\lambda_{kq} \\ & - \frac{r_{kq}L''^2_{mq}}{L^2_{lkq}}(i_{sq1} + i_{sq2}) \end{aligned}, \tag{27}$$

where the sub-transient fluxes are defined as:

$$\lambda''_{d1} = \lambda''_{d2} = \frac{L''_{md}}{L_{lkd}}\lambda_{kd} + \frac{L''_{md}}{L_{lfd}}\lambda_{fd}, \tag{28}$$

$$\lambda''_{q1} = \lambda''_{q2} = \frac{L''_{mq}}{L_{lkq}}\lambda_{kq}. \tag{29}$$

Using equations (19)-(21) and (24)-(27) the following state-variable model can be obtained:

$$\begin{aligned} & p\begin{bmatrix} \lambda_{kd} \\ \lambda_{fd} \\ \lambda_{kq} \end{bmatrix} = \mathbf{A}\begin{bmatrix} \lambda_{kd} \\ \lambda_{fd} \\ \lambda_{kq} \end{bmatrix} - \mathbf{B}\begin{bmatrix} i_{sd1} \\ i_{sq1} \\ i_{sd2} \\ i_{sq2} \\ v_{fd} \end{bmatrix}, \\ & \begin{bmatrix} e''_{sd1} \\ e''_{sq1} \\ e''_{sd2} \\ e''_{sq2} \end{bmatrix} = \mathbf{C}\begin{bmatrix} \lambda_{kd} \\ \lambda_{fd} \\ \lambda_{kq} \end{bmatrix} + \mathbf{D}\begin{bmatrix} i_{sd1} \\ i_{sq1} \\ i_{sd2} \\ i_{sq2} \\ v_{fd} \end{bmatrix} \end{aligned} \tag{30}$$

where the system matrices are defined as the following:

$$\mathbf{A} = \begin{bmatrix} \frac{r_{kd}}{L_{lkd}}\left(\frac{L''_{md}}{L_{lkd}} - 1\right) & \frac{r_{kd}L''_{md}}{L_{lfd}L_{lkd}} & 0 \\ \frac{r_{fd}L''_{md}}{L_{lfd}L_{lkd}} & \frac{r_{fd}}{L_{lfd}}\left(\frac{L''_{md}}{L_{lfd}} - 1\right) & 0 \\ 0 & 0 & \frac{r_{kq}}{L_{lkq}}\left(\frac{L''_{mq}}{L_{lkq}} - 1\right) \end{bmatrix}, \tag{31}$$

$$
\mathbf{B}=\begin{bmatrix}
-\dfrac{r_{kd}L''_{md}}{L_{lkd}} & 0 & -\dfrac{r_{kd}L''_{md}}{L_{lkd}} & 0 & 0\\
-\dfrac{r_{fd}L''_{md}}{L_{lfd}} & 0 & -\dfrac{r_{fd}L''_{md}}{L_{lfd}} & 0 & 1\\
0 & -\dfrac{r_{kq}L''_{mq}}{L_{lkq}} & 0 & -\dfrac{r_{kq}L''_{mq}}{L_{lkq}} & 0
\end{bmatrix}, \tag{32}
$$

$$
\mathbf{C}=\begin{bmatrix}
\left(\dfrac{r_{kd}L''^{2}_{md}}{L^{3}_{lkd}}-\dfrac{r_{kd}L''_{md}}{L^{2}_{lkd}}+\dfrac{r_{fd}L''^{2}_{md}}{L_{lkd}L^{2}_{lfd}}\right) & \left(\dfrac{r_{fd}L''^{2}_{md}}{L^{3}_{lfd}}-\dfrac{r_{fd}L''_{md}}{L^{2}_{lfd}}+\dfrac{r_{kd}L''^{2}_{md}}{L_{lfd}L^{2}_{lkd}}\right) & -\dfrac{\omega_r L''_{mq}}{L_{lkq}}\\
\dfrac{\omega_r L''_{md}}{L_{lkd}} & \dfrac{\omega_r L''_{md}}{L_{lfd}} & \dfrac{r_{kq}L''_{mq}}{L^{2}_{lkq}}\left(\dfrac{L''_{mq}}{L_{lkq}}-1\right)\\
\left(\dfrac{r_{kd}L''^{2}_{md}}{L^{3}_{lkd}}-\dfrac{r_{kd}L''_{md}}{L^{2}_{lkd}}+\dfrac{r_{fd}L''^{2}_{md}}{L_{lkd}L^{2}_{lfd}}\right) & \left(\dfrac{r_{fd}L''^{2}_{md}}{L^{3}_{lfd}}-\dfrac{r_{fd}L''_{md}}{L^{2}_{lfd}}+\dfrac{r_{kd}L''^{2}_{md}}{L_{lfd}L^{2}_{lkd}}\right) & -\dfrac{\omega_r L''_{mq}}{L_{lkq}}\\
\dfrac{\omega_r L''_{md}}{L_{lkd}} & \dfrac{\omega_r L''_{md}}{L_{lfd}} & \dfrac{r_{kq}L''_{mq}}{L^{2}_{lkq}}\left(\dfrac{L''_{mq}}{L_{lkq}}-1\right)
\end{bmatrix}, \tag{33}
$$

$$
\mathbf{D}=\begin{bmatrix}
-\dfrac{r_{kd}L''^{2}_{md}}{L^{2}_{lkd}}-\dfrac{r_{fd}L''^{2}_{md}}{L^{2}_{lfd}} & 0 & -\dfrac{r_{kd}L''^{2}_{md}}{L^{2}_{lkd}}-\dfrac{r_{fd}L''^{2}_{md}}{L^{2}_{lfd}} & 0 & \dfrac{L''_{md}}{L_{lfd}}\\
0 & -\dfrac{r_{kq}L''^{2}_{mq}}{L^{2}_{lkq}} & 0 & -\dfrac{r_{kq}L''^{2}_{mq}}{L^{2}_{lkq}} & 0\\
-\dfrac{r_{kd}L''^{2}_{md}}{L^{2}_{lkd}}-\dfrac{r_{fd}L''^{2}_{md}}{L^{2}_{lfd}} & 0 & -\dfrac{r_{kd}L''^{2}_{md}}{L^{2}_{lkd}}-\dfrac{r_{fd}L''^{2}_{md}}{L^{2}_{lfd}} & 0 & \dfrac{L''_{md}}{L_{lfd}}\\
0 & -\dfrac{r_{kq}L''^{2}_{mq}}{L^{2}_{lkq}} & 0 & -\dfrac{r_{kq}L''^{2}_{mq}}{L^{2}_{lkq}} & 0
\end{bmatrix}, \tag{34}
$$

Applying inverse transformation on (22) back to the six-phase system yields the following equation for the machine which can be easily interfaced with an inductive or power electronics network.

$$
\mathbf{v}_{abc1abc2}=-r_s\mathbf{i}_{abc1abc2}-p(\overline{\mathbf{K}}(\theta_r)^{-1}\mathbf{L}''_{dq12}\overline{\mathbf{K}}(\theta_r)\mathbf{i}_{abc1abc2}) +\mathbf{e}_{abc1abc2} \tag{35}
$$

III. Case Study And Simulation Results

The presented VBR model is applied to a six-phase machine with 30 degree phase shift between the two three phase winding sets. The machine feeds a six-phase system through an inductive line. The detailed electrical system in Fig. 3. is implemented in Matlab/Simulink [4] Using PLECS [3] toolbox. The simulations use ***ode45*** variable time step solver with relative and absolute error tolerances set at 10^{-4}. For benchmarking purpose, three machine models have been implemented: the conventional *qd* model, the coupled circuit phase domain model and the presented VBR model. The results obtained with each model are compared with a reference solution. The reference solution uses a CCPD model with relative and absolute error tolerances set at 10^{-7} and the maximum step size of 20µs. It should be noted that snubber resistors ($R_{snubber}$ = 40 Ω) are connected in parallel with the qd model to allow interfacing with an inductive network. The simulation runs for a 1.5 second scenario in which a single phase fault occurs on phase ‘a1’ of the stator at t=0.5 s. The modeling procedure considers the effect of mutual leakage inductances present between the phase conductors in stator slots in the machine. In order to better show the effects of these inductances, transient analysis is done both with and without the presence of mutual leakage inductances in Fig. 6.

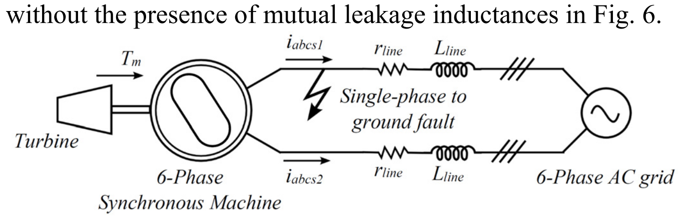

Fig. 3. Circuit schematics of the implemented system.

According to Fig. 4, all models are able to reproduce the same machine waveforms. However the models are different in terms of accuracy and simulation performance. Fig. 5. depicts a magnified view on the machine phase currents and torque immediately after the fault. According to Fig. 5. the qd model uses a significantly higher amount of time steps to achieve its solution. Due to the use of snubber resistors, the qd model solution has a considerable amount of error compared to the reference. At the same time, the other two models achieve highly accurate results with significantly less time steps with no interfacing issue.

Moreover, in order to show the importance of modeling the mutual leakage inductance in the six-phase machine, the simulation is also done for the same scenario with and without considering its effect. Fig. 6. show that the mutual inductance can have a dramatic effect on the shape and peak of the machine current wave form. While the current in the phase under fault is not affected very much, the current in the healthy phases are affected considerably according to their value of the mutual leakage inductance with the fault phase.

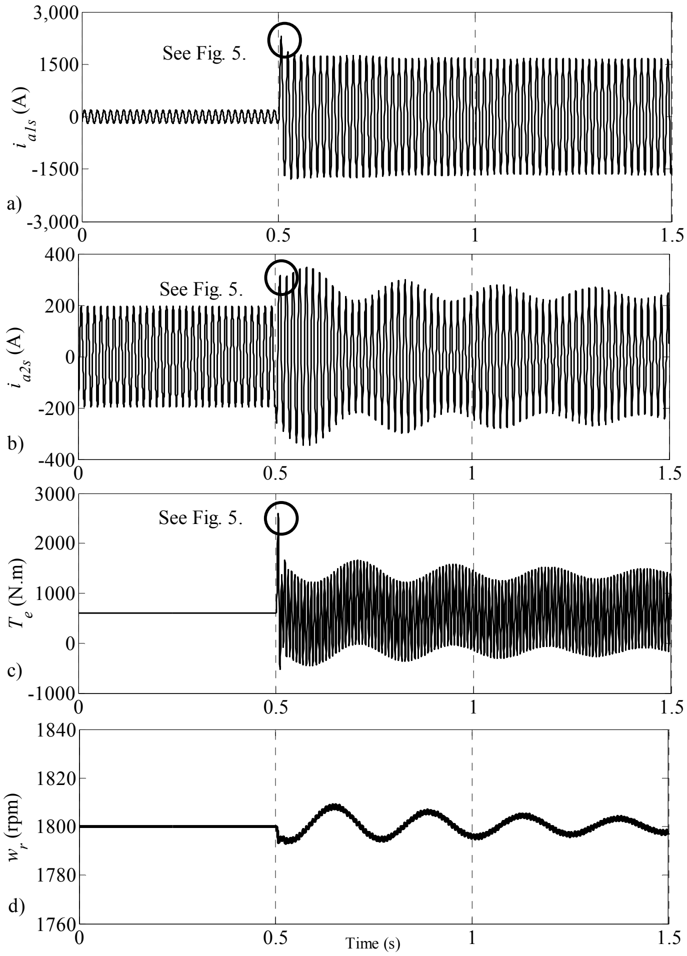

Fig. 4. The machine a) stator phase 'a1' current b) stator phase 'a2' current c) Electromagnetic torque and d) rotor speed.

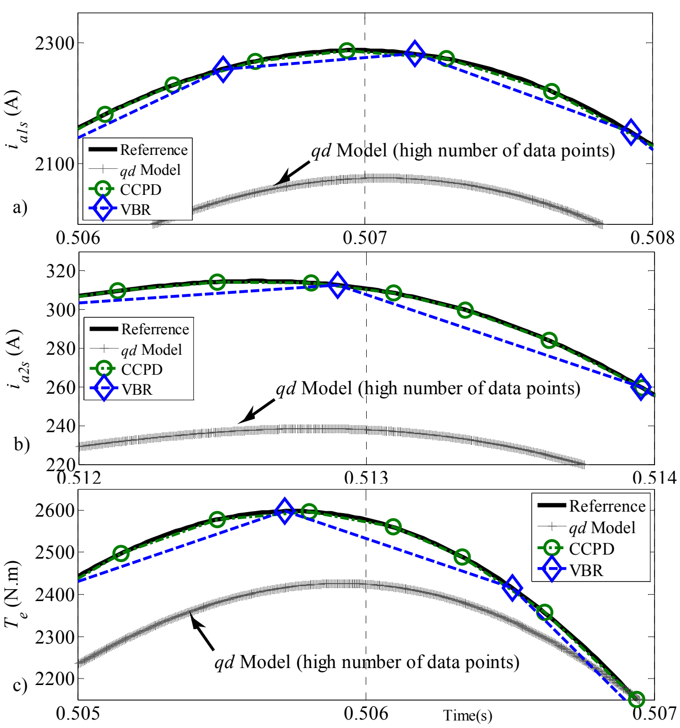

Fig. 5. Magnified view of a) stator phase 'a1' current b) stator phase 'a2' current and c) the machine torque using the implemented models.

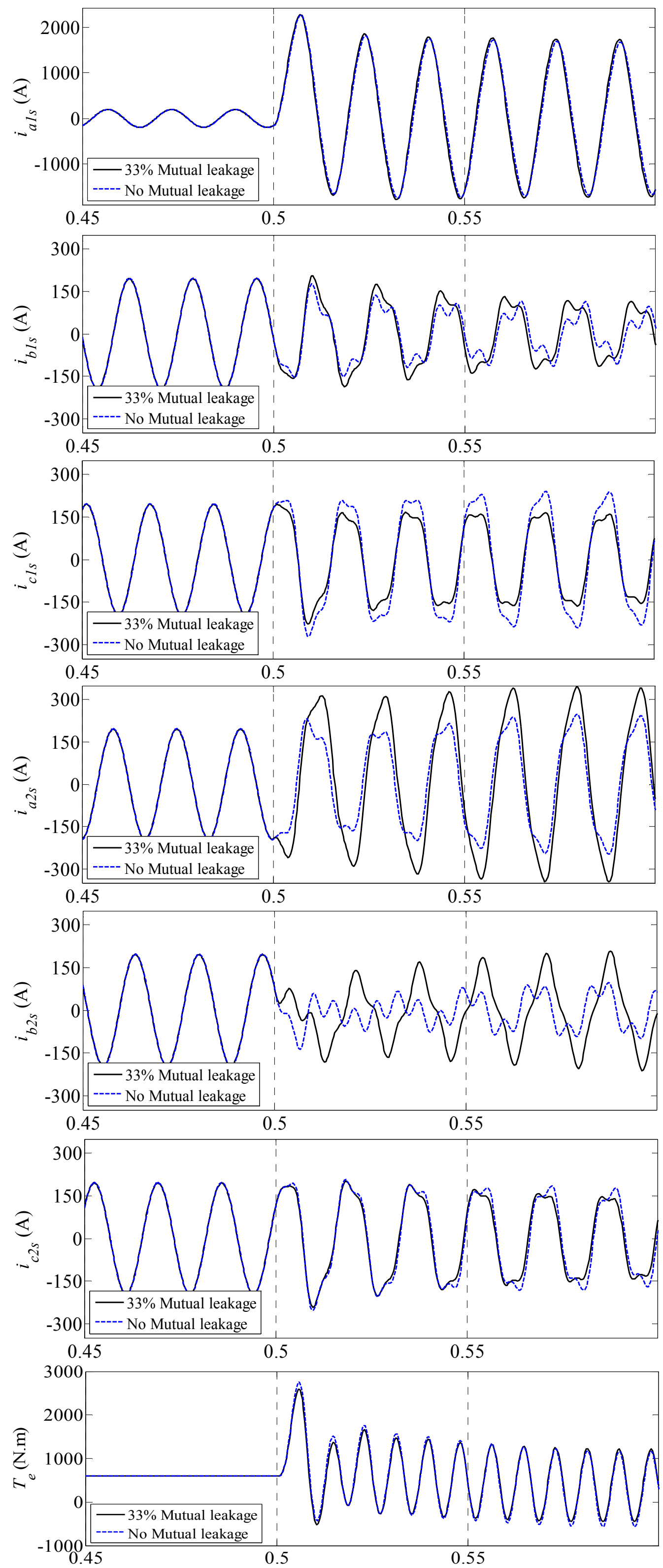

Fig. 6. Stator six phase currents at the moment of a single phase fault on phase 'a1' at t = 0.5s, with and without considering the mutual leakage inductances.

The Simulation performance in terms of CPU time and number of steps are presented in table I. It can be observed that the conventional qd model takes the highest number of steps (312,863) and CPU time (21.7s) due to high stiffness created by the snubber resistances. The CCPD model does not need snubber resistances in order to interface with an inductive system and therefore solves the system in the simulation scenario in considerably less amount of CPU time (3.9s) and lower number of time steps (6,309) due to slower system eigenvalues. However, the CCPD model still needs to solve a 9 by 9 matrix at every time step which has a negative effect on its performance. The VBR model on the other hand increases the simulation performance even more by reducing the size of the system to a 6 by 6 matrix, resulting in a CPU time of 1.1s and 1,541 for the total number of time steps.

Table II also shows very high accuracy of the CCPD and VBR model in comparison with the conventional *qd* model.

According to Fig. 6. it has been also shown that mutual leakage inductance between the conductors can affect the results considerably, especially in high current transients.

TABLE I. CPU TIME AND NUMBER OF STEPS FOR THE 1.5-SECOND STUDY

Model / Performance	Simulation Time	Number of steps
qd model with snubbers	21.7 s	312,863
CCPD model	3.9 s	6,309
VBR model	1.1 s	1,541

TABLE II. COMPARISON OF 2-NORM ERRORS

Model / Performance	2-norm of relative errors		
	Stator Current	***Electromagnetic Torque***	***Stator Voltage***
qd model with snubbers	5.06 %	4.2 %	6.56 %
CCPD model	0.04 %	0.05 %	1.8 %
VBR model	0.04 %	0.05 %	1.8 %

IV. CONCLUSIONS

In this paper a voltage behind reactance model of a six phase synchronous machine along with rotor damper windings is presented. The modeling procedure accounts for the mutual leakage inductances which are shown to have considerable effects on the final results during transients. The machine model is connected to a six-phase grid. The simulation is run for a single-phase to ground fault scenario in a 1.5 second time window. The VBR model is shown to be able to significantly outperform the conventional qd model due to lack of snubber resistances. The VBR model could also achieve better performance compared to the CCPD model due to reduced size of the system matrix.

APPENDIX

TABLE III. MACHINE PARAMETERS [14]

Parameters	Value
Rated Phase Voltage / Power	240 V / 100 kva
Rated Rotor Speed / Torque	1800 rpm / 530 N.m
L_{md}, L_{mq} , L_{ls}	3 mH , 1.4 mH , 150 µH
L_{lfd} , L_{lkq} , L_{lkd}	120 µH , 180 µH , 140 µH
r_s , r_{rkq} , r_{rkd} , r_{fd}	16 mΩ , 2.5 mΩ , 2.3 mΩ , 1.6 mΩ
L_{a1a2} , L_{a1b2} , L_{a1c2}	43 µH , -43 µH , 0 H
r_{line} , L_{line}	0.1 Ω , 100 µH

REFERENCES

[1] E. Levi, “Multiphase electric machines for variable-speed applications,” *IEEE Trans. Ind. Electron.*, vol. 55, no. 5, pp. 1893–1909, May 2008.

[2] EMTP-RV. Electromagnetic transients program. CEA Technologies, Inc., Montreal, Canada. http://www.emtp.com/.

[3] *Piecewise Linear Electrical Circuit Simulation (PLECS) User Manual*, Version 1.5, Plexim GmbH, 2006. Available: www.plexim.com

[4] MATLAB 7 (R2009 a), The MathWorks Inc., Natick, MA, USA, 2009.

[5] L. Parsa and H. A. Toliyat, “Fault-tolerant five-phase permanent magnet motor drives,” in *Conf. Rec. IEEE IAS Annu. Meeting*, Seattle,WA, 2004, pp. 1048–1054.

[6] G. J. Atkinson, B. C. Mecrow, A. G. Jack, D. J. Atkinson, P. Sangha, and M. Benarous, “The analysis of losses in high-power fault-tolerant machines for aerospace applications,” *IEEE Trans. Ind. Appl.*, vol. 42, no. 5, pp. 1162–1170, Sep./Oct. 2006.

[7] C. L. Ferreira and R. W. G. Bucknall, “Modelling and real-time simulation of an advanced marine full-electrical propulsion system,” in *Proc. IEE PEMD Conf.*, Edinburgh, U.K., 2004, pp. 574–579.

[8] E. Levi, M. Jones, S. N. Vukosavic,"A series-connected two-motor six-phase drive with induction and permanent magnet machines," *IEEE Trans. Energy Convers.*, vol.21, no.1, pp. 121-129, March 2006.

[9] C. Brandao Jacobina, V. F. Moura Bezerra Melo, N. Rocha, E. R. Cabral da Silva, "Six-Phase Machine Conversion System With Three- and Single-Phase Series Converters," *IEEE Trans. Ind. Appl.*, vol.50, no.6, pp. 3846-3856, Nov.-Dec. 2014.

[10] J. Figueroa, J. Cros, and P. Viarouge, “Generalized transformations for polyphase phase-modulation motors,” *IEEE Trans. Energy Convers.*, vol. 21, no. 2, pp. 332–341, Jun. 2006.

[11] D. C. White and H. H.Woodson, *Electromechanical Energy Conversion*. New York: Wiley, 1959.

[12] R. H. Nelson and P. C. Krause, “Induction machine analysis for arbitrary displacement between multiple winding sets,” *IEEE Trans. Power App. Syst.*, vol. PAS-93, no. 3, pp. 841–848, May 1974.

[13] J. R. Marti and K. W. Louie, “A phase-domain synchronous generator model including saturation effects,” *IEEE Trans. Power Syst.*, vol. 12, no. 1, pp. 222–229, Feb. 1997.

[14] R. F. Schiferl and C. M. Ong, “Six phase synchronous machine with AC and DC stator connections, Part I: Equivalent circuit representation and steady-state analysis,” *IEEE Trans. Power App. Syst.*, vol. PAS-102, no. 8, pp. 2685–2693, Aug. 1983.

[15] R. F. Schiferl and C. M. Ong, “Six phase synchronous machine with AC and DC stator connections, Part II: Harmonic studies and a proposed uninterruptible power supply scheme,” *IEEE Trans. Power App. Syst.*, vol. PAS-102, no. 8, pp. 2694–2701, Aug. 1983.

[16] P. C. Krause, O. Wasynczuk, and S. D. Sudhoff, *Analysis of Electric Machinery and Drive Systems*, 2nd ed. Piscataway, NJ, USA: IEEE Press, 2002.

[17] S. D. Pekarek, O. Wasynczuk, and H. J.Hegner, “An efficient and accurate model for the simulation and analysis of synchronous machine/converter systems,” *IEEE Trans. Energy Convers.*, vol. 13, no. 1, pp. 42–48, Mar. 1998.

[18] A. M. Cramer, B. P. Loop, and D. C. Aliprantis, “Synchronous machine model with voltage-behind-reactance formulation of stator and field windings,” *IEEE Trans. Energy Convers.*, vol. 27, no. 2, pp. 391–402, Jun. 2012.